Chronic treatment with fluoxetine downregulates mitochondrial activity in parvalbumin interneurons of prefrontal cortex

Abbreviated title: Flx PFC TRAP

Elias Jetsonen[1], Ilida Suleymanova[2], Eero Castren[1*], Juzoh Umemori[1, 3*]

1 Neuroscience Center, HiLIFE, University of Helsinki, Finland.

2 Faculty of Biological and Environmental Sciences, University of Helsinki, Finland

3 Gene and cell technology, A.I. Virtanen Institute, University of Eastern Finland

Shared Corresponding Authors:

Eero Castren, MD, PhD

Neuroscience Center, HiLIFE, University of Helsinki, Finland

Email: eero.castren@helsinki.fi

Address: University of Helsinki, P.O. Box 56, 00014 Helsinki, Finland

Juzoh Umemori, PhD

Neuroscience Center, HiLIFE, University of Helsinki, Finland

Gene and Cell Technology, A.I. Virtanen Institute, University of Eastern Finland

Email: juzoh.umemori@uef.fi

Address: A.I. Virtanen Institute, P.O. Box 1627, 70211 Kuopio, Finland

Abstract

Chronic treatment with fluoxetine, a widely prescribed selective serotonin reuptake inhibitor (SSRI), is known to promote neural plasticity through the activation of the neurotrophic receptor TrkB. Our previous studies have highlighted the role of TrkB in parvalbumin-positive interneurons (PV-INs) in mediating plasticity-related behaviors in the visual cortex and hippocampus. However, the impact of TrkB activity on gene expression and neuronal functions in the prefrontal cortex (PFC) remains unclear. This study aimed to investigate the effects of chronic fluoxetine on PV-INs in the PFC. Using Translating Ribosome Affinity Purification (TRAP), we found that fluoxetine treatment downregulated pathways involved in mitochondrial energy production, including NADH dehydrogenase and cytochrome c activity. Upregulated genes were associated with phosphatase activity, voltage-gated potassium channels, and amino acid transmembrane transport. Analysis of mitochondrial function specific in PV-INs revealed a reduction in mitochondrial membrane potential, while non-PV-INs in the PFC exhibited increased membrane potential. These findings suggest that fluoxetine selectively inactivates PV-INs in the PFC, leading to compensatory increases in mitochondrial activity in non-PV-INs. Immunohistochemical analyses further demonstrated reduced PV expression and weakened perineuronal nets in specific PFC regions. Our results underscore the differential impact of chronic fluoxetine on gene expression and mitochondrial function in PV-INs, suggesting region-specific disinhibition and enhanced plasticity in the PFC.

Keywords

Parvalbumin interneurons, SSRI, neural plasticity, cell-type specific transcriptome, mitochondria, BDNF, TrkB

48 **Introduction**

49 Fluoxetine is a widely used antidepressant belonging to the pharmacological group of selective
50 serotonin reuptake inhibitors (SSRI). Preclinical studies have shown that fluoxetine induces juvenile
51 like plasticity in adult rodent brain [1,2]. This has been shown to function in different neural systems,
52 like visual cortex [3], fear conditioning network [4] and reversal learning [5]. In addition, fluoxetine
53 has been shown to restore impaired neurogenesis in rodent hippocampus [6]. Mechanistically,
54 antidepressants have been shown to directly bind to neurotrophic receptor tyrosine kinase (NTRK2,
55 or TrkB) and stabilize its dimer to enhance BDNF signaling through TrkB [7].

56 Parvalbumin positive interneurons (PV-INs), are one of the largest populations of GABAergic
57 interneurons that synchronize local circuit neural activity [8], have a key role in gamma oscillations
58 [9], and are known to control neural plasticity [10]. Specifically, our studies with conditional knockout
59 mice and optogenetics demonstrated that TrkB-receptor in PV-INs is necessary and sufficient for
60 cortical plasticity in the visual cortex [11]. In addition, heterozygous removal of TrkB in PV-cells blunts
61 fluoxetine effect on reversal learning [5]. Most of PV-cells are surrounded by a specific extracellular
62 matrix formation called perineuronal net (PNN), which stabilizes synaptic connections and restricts
63 neural plasticity, particularly after critical periods of development [12]. The PNN is composed of
64 hyaluronan, chondroitin sulfate proteoglycans and linking proteins, and it surrounds soma and
65 proximal dendrites of PV-INs [13]. Enzymatic removal of the PNN has been shown to enhance
66 synaptic remodeling and restore juvenile-like plasticity, allowing for increased adaptability in neural
67 circuits [14–16]. Previous studies have demonstrated that chronic fluoxetine treatment or activation
68 of TrkB in PV-INs reduces PNN formation [4,5,11,17,18]. PV-INs play a crucial role in maintaining the
69 excitatory-inhibitory balance (E/I-balance) and optimizing synchronized signal processing in cortex
70 [19]. Notably, mature PNN reduce the E/I-balance by blocking AMPA receptor trafficking [20],
71 inhibiting TrkB activity [21], and influencing the firing potential of PV-INs [22]. The process of
72 increasing E/I-balance, known as disinhibition, has been observed to following administration of
73 venlafaxine [23], or optical activation of TrkB in PV-INs [11].

Mitochondria generate the major of cellular energy, primarily in the form of ATP, through oxidative phosphorylation, a process essential for neuronal plasticity, including synaptic transmission and memory formation [24,25]. This process begins with the oxidation of pyruvate in the Krebs cycle, which produces NADH. NADH donates electrons to the electron transport chain, driving pumping of protons across the inner mitochondrial membrane and produces a membrane potential. This membrane potential is then utilized to produce ATP on the mitochondrial membrane. Cytochrome C, a key component of electron transport chain, plays a crucial role in this process and serves as a marker for neuronal metabolic activity [26]. In addition, Translocase of the Outer Membrane 22 (Tomm22), a critical component of the mitochondrial import machinery, plays a pivotal role in maintaining mitochondrial function by facilitating the import of nuclear-encoded proteins and regulating mitophagy [27,28].

Previous studies have indicated that fluoxetine can affect mitochondrial function in neurons, although the findings have been inconsistent, with both upregulation and downregulation reported following acute or chronic administration [29]. For instance, a proteomic study from rat hippocampus found upregulation of proteins related to mitochondrial energy production [30]. In contrast, other studies observed that fluoxetine reduced mitochondrial respiration and ATP synthesis, particularly at high concentrations [31,32]. Agostinho et al also found that chronic fluoxetine decreased the activity of complex IV in the hippocampus [33]. These discrepancies likely arise from the heterogeneity of neural tissues and the diversity of cell types. However, cell-type specific analyses have not been conducted yet.

The prefrontal cortex (PFC), a functionally diverse brain region critical for decision-making, emotional regulation, and motor planning, with its connections to multiple subcortical and cortical regions [34], including midbrain, which modulate reward processing, motivation, and cognitive function [35] and the hippocampus and amygdala which are shaping network configurations essential for cognitive flexibility and emotional processing [36]. Within the PFC, the prelimbic area (PL) is primarily involved in emotional processing and the expression of fear, while the infralimbic

area (IL) is crucial for fear extinction and emotional inhibition, both of which are essential for adaptive behavior [37,38]. The anterior cingulate area (ACA), along with the supplementary motor cortex (M2), plays a central role in cognitive control, error monitoring, and motor planning, supporting cognitive flexibility and motor adaptation [39]. However, the distinctive effects of chronic treatment of fluoxetine on the different PFC areas remain elusive.

We previously conducted a transcriptomic analysis specifically for PV-INs in the hippocampus using translating ribosome affinity purification (TRAP) after a chronic treatment with fluoxetine, and found changes in gene expression, such as formation of PNNs and synaptic formations[5]. In this study, we perform the TRAP in prefrontal cortex. We found an upregulation of PV-INS plasticity-related genes and downregulation of mitochondria-related genes. Then we analyzed PV-INs specific mitochondrial functions by sorted PV-INs and then immunohistochemically analyzed mitochondrial mass and PNN formation on each subarea in the PFC.

Material and Methods

Mice

For the TRAP, transgenic mice expressing FLEX-L10a conjugating GFP [3] specifically in PV+ interneurons were produced by mating females from an homozygous PV specific Cre line [1] ($PV^{cre/cre}$; Pvalb-IRES-Cre, JAX: 008069, Jackson laboratory)[40] with males from an homozygous mice expressing GFP-L10a (Liu et al, 2014) (B6;129S4-Gt(ROSA)26Sor $^{tm9(EGFP/Rpl10a)Amc}$/J, 024750, Jackson laboratory) . For PV-INs specific mitochondria analysis, by crossing male transgenic mice harboring double inverted openreading frame (DIO)-expressing tdTomato (B6.Cg-*Gt(ROSA)26Sor*$^{tm14(CAG-tdTomato)Hze}$/J, RRID:IMSR_JAX:007914, Jackson laboratory) [41] with female mice of the homozygous PV specific Cre line ($PV^{cre/cre}$)[40].

All mice were kept in a room at 23±2°C with a 12-hr light/dark cycle (lights on at 6:00 a.m.) with access to food and water ad libitum. Three months old male mice are used for this study. All experiments were carried out in accordance with the European Communities Council Directive

126 86/6609/EEC and the guidelines of the Society for Neuroscience and were approved by the County
127 Administrative Board of Southern Finland (License number: ESAVI/38503/2019).
128
129 Fluoxetine treatment
130 0.008 % solution of fluoxetine was administered in drinking water for 14 days in all experiments. For
131 both control and treated groups, drinking water included 0.1 % saccharine for equalizing taste of
132 water. The same treatment conditions were used for all experiments.
133
134 TRAP
135 TRAP analysis was performed according to previously published protocol [42]. Briefly, we isolated
136 prefrontal cortex (PFC) from mice expressing GFP tag in ribosomes of PV-cells, as mentioned above.
137 The isolated PFC were stored in -80 C between isolation and TRAP analysis. After lysating the PFC, the
138 tagged ribosomes were precipitated using magnetic beads coated with anti-GFP antibodies. Quality
139 of RNA was assessed by Bioanalyzer (Agilent, California, US), and one sample was excluded due to
140 low RNA integrity (2.4 while it was between 7.6-9.5) (Supplemental fig 2). Actively translated mRNA
141 co-precipitated and were sequenced using HiSeq2500 (Illumina, CA, USA) with SMART-Seq v4 Ultra
142 Low Input RNA kit (Takara, Japan) for making cDNA library.
143
144 ATP assay
145 PV-TdT mice were anesthetized with pentobarbital and transcardially perfused. The brains were
146 removed, and hippocampus, prefrontal cortex and other parts of the cortex were dissected. Cells
147 were dissociated using Neural Tissue Dissociation Kit (Miltenyi, Germany) according to
148 manufacturer's protocol. The cells were then FACS sorted to PV and non-PV cells based on TdT
149 expression. ATP was detected using CellTiter (Promega, Wisconsin US) according to manufacturer's
150 protocol. Luminescence was detected with Varioskan Flash (Thermo Fisher, Massachusetts US).
151

152 Mitochondrial mass and membrane potential assay

153 PV-TdT mice were anesthetized using pentobarbital and transcardially perfused with cooled N-
154 methyl-D-glucamine buffer to preserve cells. Brains were isolated and hippocampus, prefrontal
155 cortex and rest of the cortex were dissected. Cells were dissociated using Neural Tissue Dissociation
156 Kit (Miltenyi, Germany) according to manufacturer's protocol. The cells were then FACS sorted to PV
157 and non-PV cells based on TdT expression. To measure mitochondrial mass, the cells were stained
158 with MitoTracker Green (Thermo Fisher, Massachusetts US) for 30 min in 37 C. To measure
159 mitochondrial membrane potential, the cells were stained with 5 nm Rhodamine 123 [43], for 30 min
160 in +4 C. The cells were centrifuged at 300 g for 10 min and diluted with D-PBS before proceeding to
161 the second round of FACS. During sorting, fluorescence was measured for each cell.

162

163 Immunohistochemistry on PV, PNN and TOMM22

164 Mice were deeply anesthetized and perfused with 4 % PFA in PBS. The brains were cut into 40 µm
165 sections and stored in +4 °C until further processing. Sections were then washed with PBST and
166 blocked using bovine serum albumin and donkey serum. The sections were stained with primary
167 antibodies overnight and, after additional PBST washing, secondary antibodies for 1 h in room
168 temperature. Details of used antibodies and their dilutions are listed on table. Images were obtained
169 using Andor Dragonfly (Oxford Instruments, United Kingdom).

170

171 **Imaging analysis**

172 The whole PFC was imaged on multiple frames and Z-stack. Images were stitched using ImageJ and
173 the best layer of Z-stack was manually selected for analysis. Subregions were identified using a
174 reference atlas [44]. Cell borders were detected using customized scripts based on morphological
175 features and thresholding using Matlab (The MathWorks, Massachusetts, US). Cells were detected
176 using PV and PNN staining, and data of overlapping cells was combined. PV and TOMM22 signal

intensities were measured in cells detected by PV shape and PNN signal intensity was measured in cells detected by PNN shape.

Experimental design and statistical analysis

Statistical analysis for TRAP was conducted using R and package DESeq2 [45]. Multiple test correction was performed using Benjamini-Hochberg procedure, and Q-value (corrected P-value) of 0.1 was considered significant. Pathway analysis was performed using package clusterProfiler [46]. Resulting pathways were clustered and visualized using the function “emapplot_cluster”.

Data for other assays in this article were analyzed by two-way ANOVA followed by post hoc test with multiple test correction using Šídák’s method, or Chi-square test when suitable. Statistical analyses were performed using Prism 9 (GraphPad Software, California, US). P-value < 0.05 was considered significant.

191 **Results**

192 ***Identification of PV-IN specific gene expression changes following chronic fluoxetine***

193 ***treatment***

194 After two weeks of fluoxetine treatment, we performed Translating Ribosome Affinity Purification

195 (TRAP) analysis on parvalbumin-positive interneurons (PV-INs) (Fig. 1a-b). Following the application

196 the Benjamini-Hochberg procedure for multiple test correction, we identified 315 DEGs (q > 0.1) (Fig

197 1c, Supplemental table 2). 50 DEGs with lowest q-values are shown in Fig 2a.

198

199

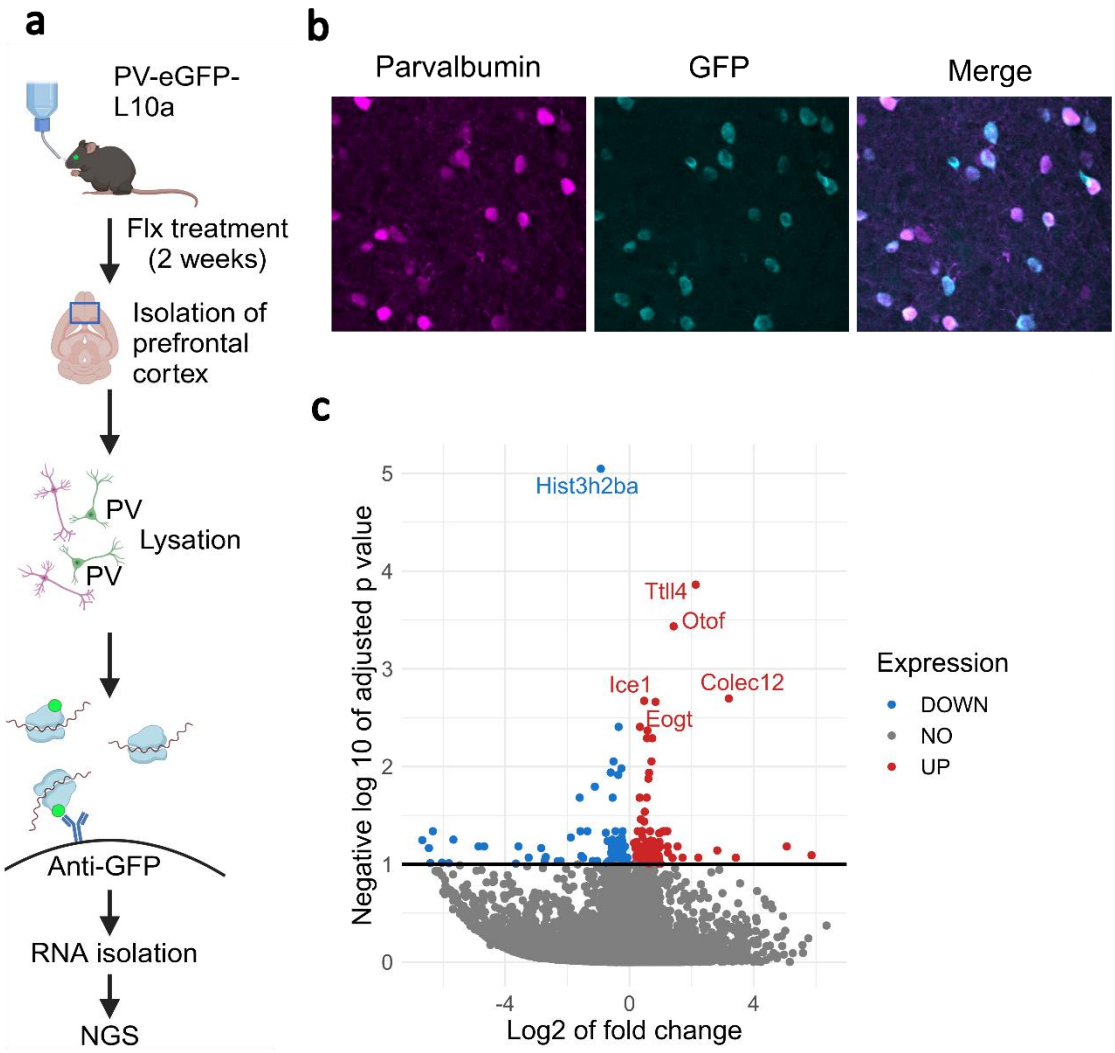

200

201 Figure 1: TRAP analysis on PV-INs.

202 **a)** PV-eGFP-L10a mice were treated with fluoxetine or water for 2 weeks, and their PFC were
203 isolated post-euthanasia. GFP-tagged translating ribosomes binding mRNA were precipitated
204 from cell lysate using magnetic beads coated with anti-GFP antibodies, enabling the isolation of
205 ribosome-bound mRNA. The isolated mRNA was then converted into cDNA and sequenced using
206 next-generation sequencing (NGS). **b)** Representative PFC section from PV-eGFP-L10a mouse
207 stained with parvalbumin antibody. GFP co-localizes with parvalbumin, confirming the specificity
208 of the PV-IN labeling **c)** Volcano plot showing differentially expressed genes in PV-INs, with the x-
209 axis representing the magnitude of change (log2 fold change) and the y-axis representing
210 statistical significance (−log10 adjusted p-value) on. Upregulated genes are highlighted in red and
211 downregulated genes in blue, providing a visual overview of the transcriptional changes induced
212 by fluoxetine.

213

214 We then conducted a pathway analysis for GO Molecular Function -pathways using these DEGs and
215 identified upregulation in 30 and downregulation of 20 functional pathways (Fig 2b and c,
216 supplemental table 3), and representative DEGs in the pathways are shown in Fig. 3. Notably, we
217 observed significant downregulation in pathways associated with mitochondrial function (Fig. 2b).
218 These included proton ATPase activity, synthesis and activity of NADH dehydrogenase (quinone), and
219 mitochondrial ribonucleoprotein ribosome complex functions. In fact, we identified the
220 downregulation of genes such as Atp5d, Cox5a, Mrpl14, Timm13, Tomm22, and Ndufa1, which are
221 crucial components of the mitochondrial electron transport chain, protein synthesis and
222 mitochondrial transmembrane transport [47]. This downregulation suggests a reduction in
223 mitochondrial energy production and efficiency, which may contribute to lowered excitatory states in
224 PV-INs post-fluoxetine treatment [11]. Additionally, we observed downregulation in pathways
225 associated with ribosomes, including Rplp1, Rps13, and Rpl17 (Fig. 3b), which are involved in
226 ribosome biogenesis and function [48,49]. These reductions implicate decreased protein synthesis,
227 and the metabolic changes observed in PV-INs may affect fundamental cellular functions and
228 metabolism.

229

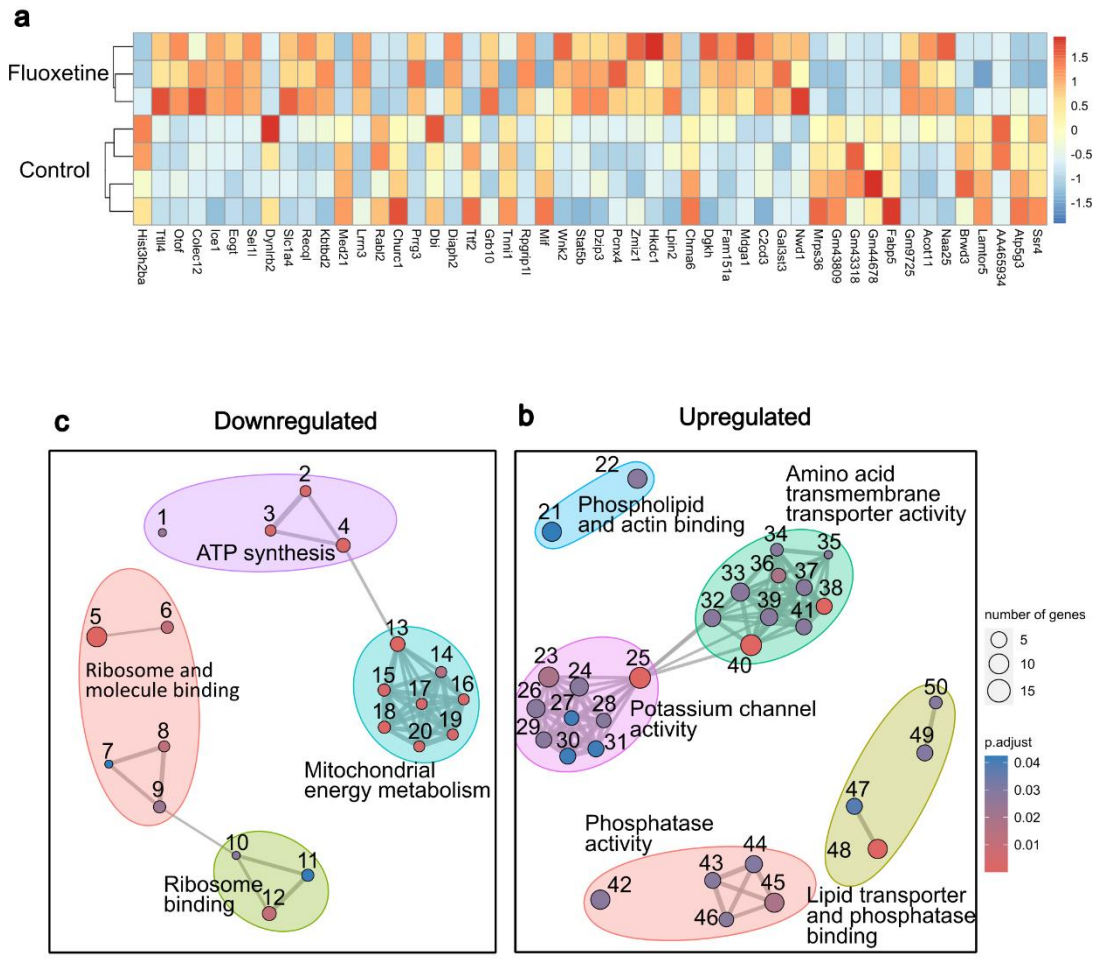

Figure 2: TRAP Analysis in PV-INs after Chronic Fluoxetine Treatment

a) Heatmap of 50 most differentially expressed genes (DEGs) in PV-INs after chronic fluoxetine treatment, illustrating the extent and pattern of gene expression changes. **b-c)** Results of pathway enrichment analysis of GO Molecular Function -pathways in PV-INs clustered into 50 subgroups. Numbers correspond to individual pathways in Supplementary table 3. **b)** Downregulated pathways predominantly involve mitochondrial energy production, including NADH dehydrogenase activity, oxidoreductase activity, cytochrome c function, electron transport, proton transmembrane transport, and ATP synthase. Additionally, downregulation of ribosome-related pathways is observed, suggesting a broad impact on cellular metabolism and protein synthesis. **c)** Upregulated pathways are related to phosphatase activity, amino acid transmembrane transport, and voltage-gated potassium channels, highlighting enhanced synaptic and signaling activities [11]. The complete details of the 50 pathways are listed in supplemental table 3.

Upregulated pathways included those related to actin binding, phosphatase activity, amino acid transmembrane transport, voltage gated potassium channel activity, and ion gated channel activity (Fig. 2c). For instance, upregulated Wnk2, Kcnf1, and Ptpn9 (Fig. 3c), are associated with ion transport and cellular signaling pathways [50], indicating enhanced cellular communication and ion homeostasis, which may contribute to altered intracellular signaling in PV-INs. Actin-binding proteins, which play a crucial role in dendritic spine formation and synaptic plasticity, were notably upregulated, consistent with previous findings linking these proteins to structural plasticity in neurons [51]. Additionally, the upregulation of voltage-gated potassium channels aligns with the modulation by brain-derived neurotrophic factor (BDNF) exposure [52] and activation of its receptor TrkB [11], which is also activated by chronic fluoxetine treatment [7,53–55]. The increased phosphatase activity, particularly involving protein dephosphorylation, suggests a role in modulating synaptic plasticity and signal transduction [56]. Furthermore, the upregulation of amino acid transport genes indicates enhanced neurotransmitter availability, which could support increased synaptic transmission and more robust neuronal communication [57].

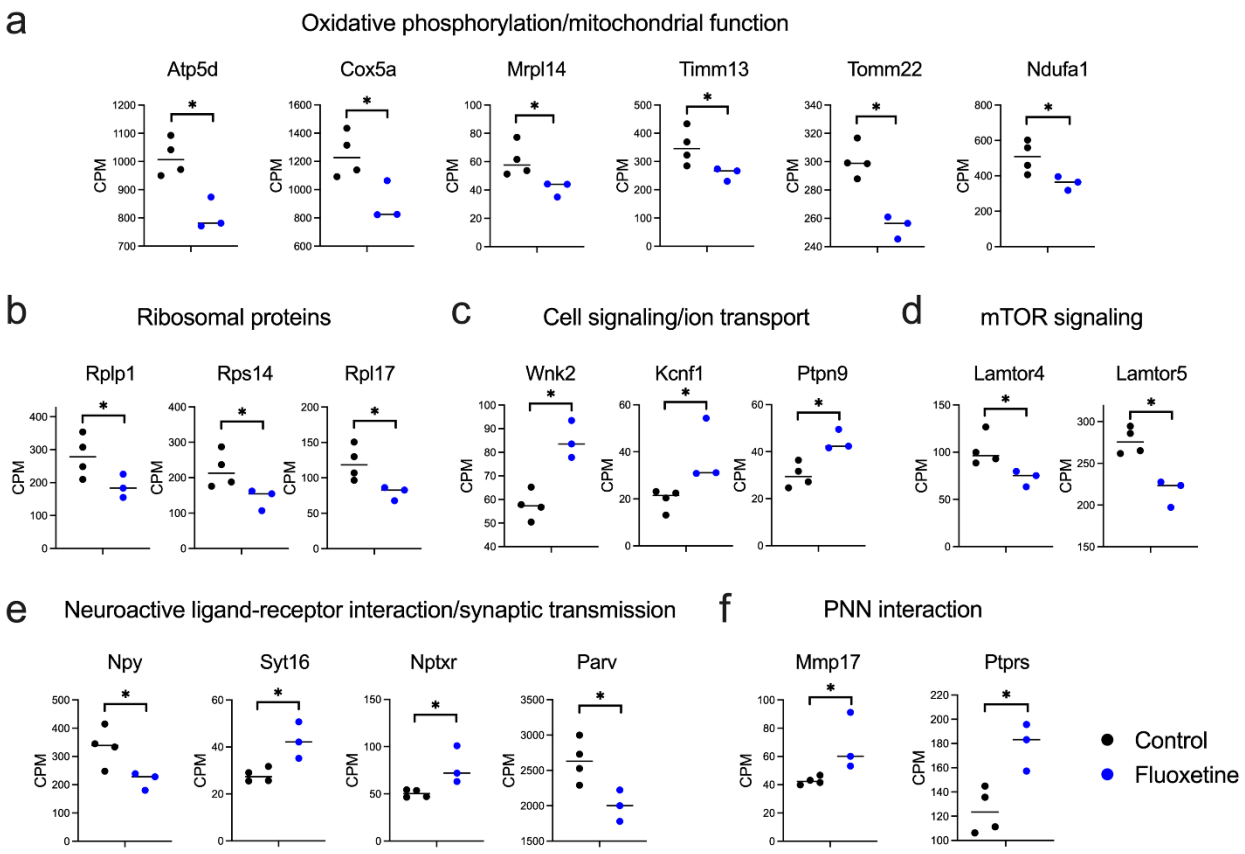

Figure 3: Representative DEGs After Chronic Fluoxetine Treatment

a) Oxidative Phosphorylation and Mitochondrial Function: Downregulated genes Atp5d, Cox5a, Mrpl14, Timm13, Tomm22, and Ndufa1 are critical components of the mitochondrial electron transport chain, protein synthesis and transmembrane transport, suggesting reduced mitochondrial activity in PV-INs. **b)** Ribosomal Proteins: Downregulated genes Rplp1, Rps13, and Rpl17 are involved in ribosome biogenesis and function, indicating a potential decrease in protein synthesis capacity. **c)** Cell Signaling/Ion Transport: Upregulated genes Wnk2, Kcnf1, and Ptpn9 are associated with ion transport and signaling pathways. **d)** mTOR Signaling and Lysosomal Function: Downregulated genes Lamtor4 and Lamtor5 are part of the mTOR signaling pathway and lysosomal function, indicating possible suppression of cellular growth and metabolism. **e)** Neuroactive Ligand-Receptor Interaction/Synaptic Transmission: Downregulated genes Npy and Parv suggest reduced inhibitory signaling and calcium buffering, potentially decreasing inhibitory tone. Upregulated genes Syt16 and Nptxr indicate enhanced synaptic transmission and receptor clustering, possibly leading to increased excitatory signaling to PV-INs and synaptic plasticity. **f)** PNN interaction: Mmp17, an upregulated gene, plays a key role in matrix remodeling and may lead to the degradation of perineuronal nets (PNNs), supporting increased synaptic flexibility and potentially facilitating structural reorganization in response to

chronic fluoxetine treatment. Receptor type protein tyrosine phosphatase (Ptprs) was upregulated. It modulates TrkB activity in interaction with PNNs and plays role in memory retention. * indicates statistical significance with $q < 0.1$.

In other pathways, downregulation of Lamtor4 and Lamtor5 within mTOR signaling and lysosomal function pathways (Fig. 3d) suggests suppression of cellular growth and metabolism, potentially reducing anabolic processes in PV-INs [58]. Additionally, downregulation of Neuropeptide Y (Npy) and Parvalbumin (Parv) (Fig. 3e) suggests weakened neuroactive ligand-receptor interaction and synaptic transmission. NPY enhances inhibitory tone and regulating stress and anxiety [59], while Parv, crucial for calcium buffering in fast-spiking interneurons, regulate neuronal excitability [60,61]. This may reduce inhibitory tone and disrupt calcium homeostasis in PV-INs. In contrast, the upregulation of Synaptotagmin 16 (Syt16) and Neuronal Pentraxin Receptor (Nptxr) suggests enhanced synaptic transmission and receptor clustering. Syt16 a member of synaptotagmin family involved in synaptic vesicle exocytosis, may play a role in synaptic function, with other synaptotagmins, such as Syt4, being implicated in BDNF release [62]. Nptxr, which regulates AMPA receptor clustering, promotes synaptic plasticity and receptor localization at synapses [63]. The upregulation may increase excitatory signaling onto PV-INs, thereby altering the E/I balance in a complex manner. Lastly, we found upregulated genes interacting with PNN (Fig. 3f), Matrix metalloproteinase-17 (Mmp17) was upregulated (Fig. 3f). MMPs degrade extracellular matrix structures, such as PNN [64], and the upregulation of Mmp17 may facilitate structural reorganization in response to chronic fluoxetine treatment, potentially modulating the activity of PV-INs [12,22]. In contrast, Receptor type protein tyrosine phosphatase sigma (Ptprs), which interacts with chondroitin sulfate proteoglycans (CSPGs) in PNNs, was upregulated (Fig. 3f). This is consistent with previous studies showing that Ptprs dephosphorylate TrkB, an interaction modulated by fluoxetine and known to play a role in memory retention [15].

304 These findings suggest that chronic fluoxetine treatment leads to a complex reorganization of
305 gene expression in PV-INs, with upregulated synaptic and neurotransmitter-related functions, while
306 simultaneously leading to reduced mitochondrial activity. This dual impact highlights the intricate
307 balance between promoting plasticity and altering cellular energy dynamics in response to
308 fluoxetine.
309
310 ***Chronic Fluoxetine Treatment Reduces Mitochondrial Membrane Potential in PV-INs***
311 To further investigate the impact of chronic fluoxetine treatment on mitochondrial function, we
312 measured mitochondrial membrane potential, mitochondrial mass and intracellular ATP contents in
313 FACS-sorted cells after chronic fluoxetine administration.
314 A key finding was a marked reduction in mitochondrial membrane potential in PV-INs across
315 all brain regions after fluoxetine treatment ($p < 0.0001$) (Fig. 4a). In contrast, an increase in
316 membrane potential was observed specifically in non-PV cells of the PFC ($p < 0,0001$) (Fig. 4d). A
317 decrease in membrane potential typically indicates a reduction in ATP production by the
318 mitochondrial electron transport chain. Mitochondrial mass in PV-INs remained elevated in the PFC
319 with no significant changes in other brain regions post-treatment (Fig. 4b). Mitochondrial mass was,
320 however, reduced in non-PV cells after fluoxetine treatment ($p = 0,0071$) (Fig. 4e). Despite the
321 reduced membrane potential, no significant changes in ATP levels were detected in any cell type,
322 including PV-INs (Fig. 4c, f). Notably, ATP levels were higher in the PFC compared to the hippocampus
323 and other cortical regions, specifically in PV-INs ($p < 0.0001$), but fluoxetine treatment did not
324 significantly affect ATP levels (Fig. 4c).
325 These results suggest that while mitochondrial energy production remains active in PFC,
326 chronic fluoxetine treatment reduces energy production in PV-INs without alternating intracellular
327 ATP levels or mitochondrial mass. This reduction in PV-INs may contribute to the disinhibition of
328 other cortical cell types, particularly excitatory neurons, which could be reflected in the upregulation
329 of their energy production in non-PV-INs.

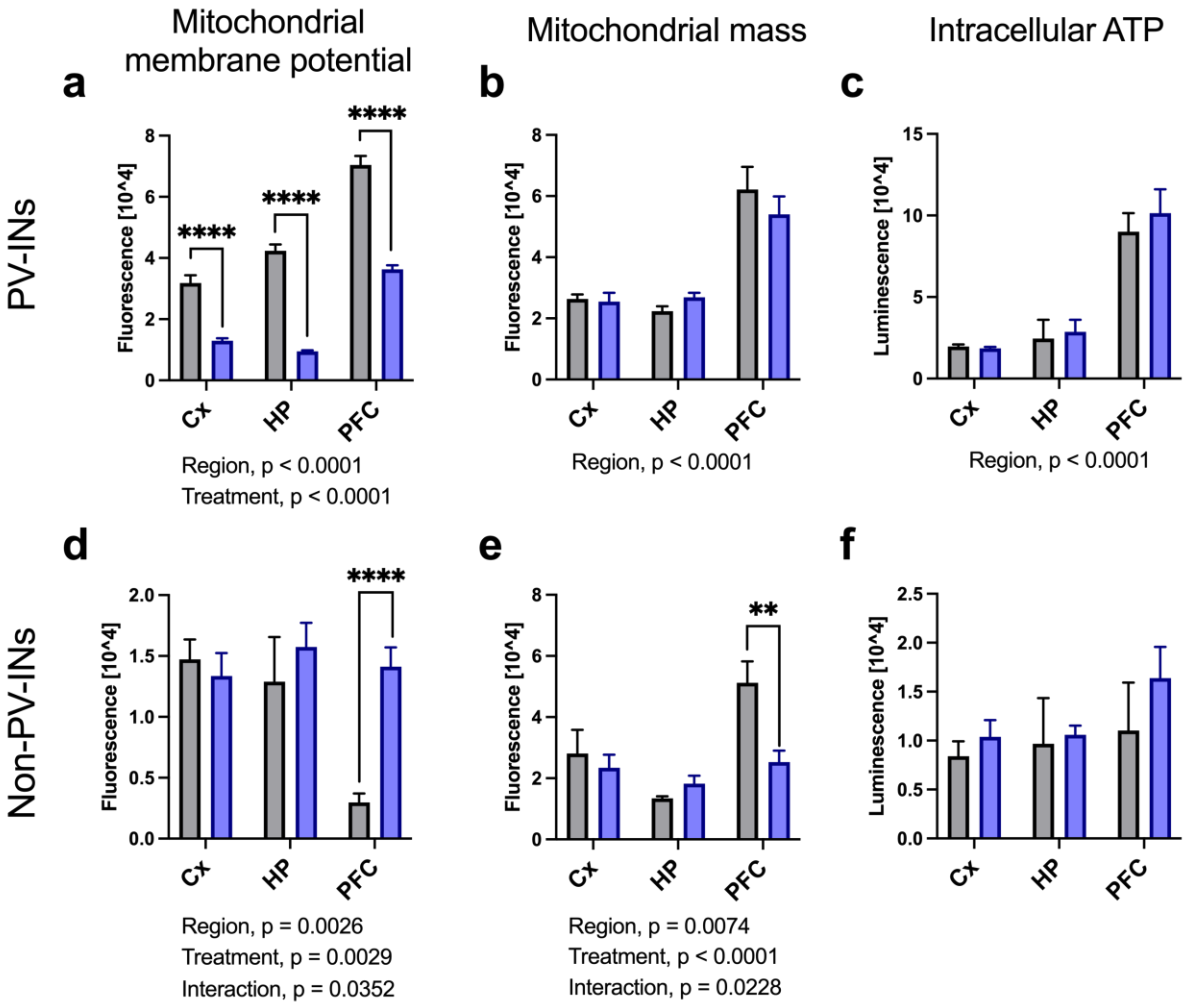

Figure 4: ATP production and mitochondria assays using FACS-sorted cells.

PV and other types of cells were sorted and analyzed separately in the cortex (Cx), Hippocampus (HP), and prefrontal cortex (PFC): PV-INs, a, b, c; Non-PV-Cells, d, e, f. **(a, d)** Mitochondrial membrane potential was significantly downregulated in PV-INs from all studied regions (P < 0,0001). Interestingly, upregulation of mitochondrial membrane potential was shown in non-PV-INs from PFC (P < 0,0001). **(b,e)** No differences in mitochondrial mass were seen in PV-cells, while it was down-regulated in non-PV-cells from PFC (Two-way ANOVA, Treatment, F (1, 3617) = 5,191, P=0,0228; Šídák's multiple comparisons test ”control” vs ”fluoxetine”, PFC: P = 0,0071). **(c,f)** No differences in intracellular ATP were seen after fluoxetine treatment in either cell type. Bars represent standard error of means, with ANOVA results noted below each plot.

344

345 ***Chronic Fluoxetine Modulates PV Cell distribution and PNN Structure in the PFC***

346 To investigate plastic changes and mitochondrial functions in specific subregions of the prefrontal
347 cortex (PFC), we performed immunohistochemical analysis staining with antibodies of PV and PNN,
348 plastic markers of PV-INs, and TOMM22, a marker of mitochondrial mass and function (Fig 5a). The
349 analysis was focused on the prelimbic area (PL), infralimbic area (IL), and anterior cingulate area with
350 supplementary motor area (ACA/M2), based on a reference atlas [44]. There was no treatment effect
351 of fluoxetine on number of PV-INs (Fig. 5b).

352

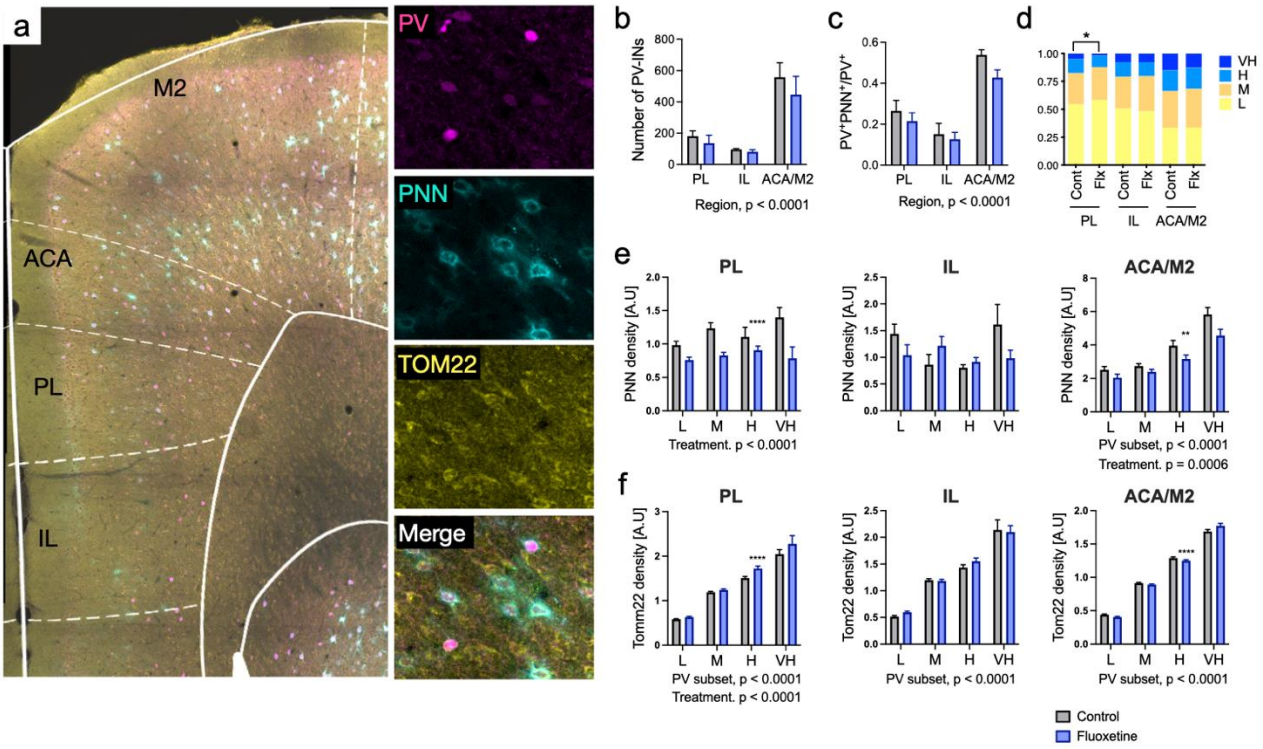

353

354 Figure 5: Immunostaining and imaging analysis PV, PNN and TOMM22in the PFC.

355 **a)** Immunostaining and imaging analysis were performed to assess parvalbumin (PV),
356 perineuronal nets (PNN), and TOMM22, a quantitative mitochondrial marker. Sub-regions of
357 the prefrontal cortex, including the infralimbic region (IL), prelimbic region (PL), and anterior
358 cingulate area with secondary motor cortex (ACA/M2), were identified using a reference
359 atlas and selected for subsequent analysis. **b)** Number of PV-INs in different subregions.

Fluoxetine treatment didn't have a significant effect on cell count. **c)** The proportion of PV-positive cells surrounded by PNN was assessed. Although no significant treatment effect was observed, the ratio of PNN-positive PV cells varied significantly between regions (two-way ANOVA, Region, $F(2, 18) = 36{,}35$ $p < 0.0001$). **d)** PV-positive cells were categorized into four subgroups based on PV expression levels. The relative number of cells expressing very high levels of PV was significantly lower in the PL region following fluoxetine treatment (Chi-square test, $p = 0.0175$). **e)** The intensity of PNNs in PV-cell subsets (low, middle, high, and very high PV expression) was analyzed after chronic fluoxetine treatment in the PL, IL, and ACA/M2 regions. In both the PL and ACA/M2 regions, fluoxetine treatment significantly reduced the overall intensity of PNNs (Two-way ANOVA, Treatment, PL: $F(1, 335) = 17{,}28$, $p < 0.0001$; ACA/M2: Treatment, $F(1, 1744) = 11{,}68$, $p = 0.0006$). Additionally, there was a significant effect of PV expression subsets (Two-way ANOVA, PV subset, ACA/M2: $F(3, 1744) = 40{,}64$, $p = 0.0006$), indicating a positive correlation between PNN intensity and PV expression in the ACA/M2 region. **f)** The intensity of TOMM22 in PV-cell subsets was also analyzed. In all regions, a significant effect of PV expression subsets was observed (Two-way ANOVA, PV subset, PL: $F(3, 1287) = 791{,}0$ $p < 0.0001$; IL: $F(3, 714) = 390{,}7$, $p < 0.0001$; ACA/M2: $F(3, 4012) = 2756$, $p < 0.0001$), indicating that PV-INs with higher PV expression exhibited higher TOMM22 levels compared to those with lower PV expression. Fluoxetine treatment significantly increased TOMM22 expression only in the PL region (Two-way ANOVA, Treatment, $F(1, 1287) = 21{,}17$, $p < 0.0001$). Bars represent standard error of means, with ANOVA results noted below each plot.

PV-positive cells were categorized into four subgroups based on PV expression levels, as previous studies have shown a negative correlation between PV expression intensity and plasticity in PV-INs [5,10,11]. Chronic fluoxetine treatment led to a significant decrease in the number of cells expressing very high levels of PV particularly in the PL region ($p = 0.0175$) (Fig. 5d), consistent with previous findings in the visual cortex [11] and hippocampus [5].

The analysis of PNNs revealed a significant reduction in total PNN intensity in both the PL and ACA/M2 regions following fluoxetine treatment (PL, $p < 0.0001$; ACA/M2, $p = 0.0006$). Additionally, there was a significant effect of PV expression subsets, with a positive correlation between PNN intensity and PV expression levels in the ACA/M2 region ($p = 0.0006$) (Fig. 5e).

391 TOMM22 intensity across PV-IN subsets showed a significant increase in TOMM22 expression only in
392 the PL region post-treatment ($p < 0.0001$) (Fig. 5e). In all regions, PV-INs with higher PV expression
393 exhibited higher TOMM22 levels than those with lower PV expression ($p < 0.0001$).
394 These results suggest that chronic fluoxetine treatment induces notable changes in PV cell
395 plasticity and PNN structure, especially in the PL and ACA/M2 regions. The reduction in the number
396 of high PV-expressing PV-INs and corresponding PNN intensity implies increased plasticity in these
397 regions. Although no overall TOMM22 loss was detected following fluoxetine treatment, as observed
398 in the TRAP analysis, the correlation between TOMM22 and PV expression suggest that high PV-
399 expressing PV-INs may have a high energy consumption.
400
401 **Discussion**
402 Here, we demonstrated that chronic fluoxetine treatment in mice induced transcriptional changes in
403 PV-INs, notably downregulating mitochondrial energy production, as observed in transcriptome data
404 and reduced mitochondrial membrane potential in PV-INs of the PFC. In contrast, non-PV-INs
405 exhibited an increase in membrane potential. Despite these changes, mitochondrial mass and ATP
406 levels remained stable, suggesting fluoxetine may reduce mitochondrial efficiency in the PFC. Altered
407 genetic pathways related to voltage-gated potassium channels, phosphatase activity, phospholipid
408 binding, and extracellular matrix remodeling indicate broader impacts on cellular communication
409 and metabolism. Immunohistochemical analysis corroborated these findings, revealing reductions in
410 PV expression and perineuronal nets (PNNs) without significant changes in TOMM22 intensity,
411 highlighting consistent mitochondrial mass. These results underscore the complexity of fluoxetine's
412 effects on PV-INs, particularly in energy metabolism and synaptic plasticity.
413
414 *Role of TrkB Activation and Synaptic Plasticity*
415 Chronic fluoxetine treatment was found to enhance TrkB activation [7], the receptor for brain-
416 derived neurotrophic factor (BDNF), which plays a pivotal role in synaptic plasticity, neuronal survival,

417 and growth [7,65], especially in PV-INs [5,11]. Our TRAP analysis identified 315 DEGs in PV-INs, with
418 notable upregulation of pathways associated with synaptic plasticity, including actin binding, voltage-
419 gated potassium channel activity, and amino acid transmembrane transport. These findings suggest
420 that fluoxetine promotes a state of enhanced plasticity in PV-INs, further supported by the observed
421 downregulation of parvalbumin and perineuronal nets (PNNs), point to a more permissive
422 environment for synaptic remodeling.
423
424 *Impact on E/I Balance and Mitochondrial Dynamics*
425 PV-INs are crucial for maintaining the excitatory/inhibitory (E/I) balance in cortical circuits, with
426 dysregulation linked to psychiatric conditions, like depression [66,67]. The downregulation of
427 parvalbumin and PNNs, coupled with reduced energy dynamics following fluoxetine treatment,
428 suggests a reduction in the inhibitory tone of PV-INs. This aligns with our previous studies showing
429 that activation of TrkB specifically in PV-INs reduces their excitability, partially through
430 downregulation of Kv3 family potassium channel activity [11]. A reduced inhibitory tone potentially
431 shifts the E/I balance towards increased excitation, enhancing the plasticity of excitatory synapses
432 and promoting the remodeling of cortical circuits required for cognitive flexibility and emotional
433 regulation [19].
434 We also observed a reduction in mitochondrial membrane potential in PV-INs while an
435 increase in non-PV-INs. As mitochondrial membrane potential is generated by electron transport
436 chain complexes I-IV and is used to produce ATP by complex V, ATP synthase [68], so our findings
437 show that energy metabolism is decreased in PV-INs and increased in non-PV-INs. This shift may
438 contribute to a disinhibition of excitatory neurons, which compose most of the non-PV-INs. Despite
439 of wide transcriptional changes and downregulation of mitochondrial membrane potential, we did
440 not observe fluoxetine effects on intracellular ATP levels, possibly due to the broad cellular functions
441 ATP supports, maintaining constant concentration, even as its production altered. Additionally,
442 technical limitations such as the sensitivity of ATP detection assays and the rapid, localized turnover

443 of ATP might have masked subtle changes. The heterogeneity of cell populations in PV-INs could
444 further dilute small ATP changes, and the dynamic nature of ATP production may require more
445 sensitive, real-time measurements. Our two-week treatment duration may have been insufficient to
446 observe mitochondrial mass changes, warranting further studies with longer treatment period.
447
448 *Region-specific modulation of PV-IN plasticity in the prefrontal cortex by chronic fluoxetine treatment*
449 Our study reveals region-specific effects of chronic fluoxetine treatment on PV-INs across key
450 subregions of PFC, aligning with their distinct roles in emotional and cognitive processing. In the PL,
451 associated with fear expression, fluoxetine reduced PV expression, suggesting enhanced plasticity
452 that may aid in emotional regulation and anxiety relief [37,38]. While no significant changes were
453 observed in the IL, critical for fear extinction, the trend toward reduced inhibitory tone could support
454 the formation of new, less fearful associations [69]. In the ACA/M2, which are involved in cognitive
455 flexibility and motor planning, reduced perineuronal net (PNN) intensity points to increased synaptic
456 remodeling, potentially enhancing adaptability and cognitive function [39]. These findings highlight
457 that fluoxetine's region-specific enhancement of plasticity in the PFC, contributing to its therapeutic
458 effects in treating depression and anxiety by modulating neural circuits related to emotion and
459 cognition.
460
461 *Clinical Implications and Future Directions*
462 The modulation of PV-INs by fluoxetine carries significant clinical implications, particularly given their
463 crucial role in maintaining cortical network balance. Fluoxetine's ability to reduce PV expression and
464 PNN density may help restore E/I balance in conditions with pathologically elevated inhibition,
465 offering therapeutic benefits in mood disorders and other neuropsychiatric conditions characterized
466 by disrupted cortical networks [8]. Our findings highlight potential biomarkers related to PV-IN
467 plasticity or mitochondrial activity, which could aid in identify new therapeutic targets. Future
468 research should focus on exploring the long-term effects of fluoxetine on neural circuitry and

469 cognitive function to better understand its full spectrum of therapeutic outcomes. Additionally,
470 translational research should investigate combining fluoxetine with psychotherapy [2] or treatments
471 targeting complementary pathways, such as synaptic stabilization [70], to enhance its efficacy and
472 broaden its applicability in treating various neuropsychiatric disorders.
473

474 Acknowledgments
475 The authors would like to thank Sulo Kolehmainen and Seija Lågas for technical help. We also thank
476 the Biomedicum Flow cytometry unit at the University of Helsinki for instructing Sony SH800Z Cell
477 Sorter. We thank Biomedicum Imaging unit at the University of Helsinki for providing equipment and
478 technical help for immunohistochemical analysis. This work was carried out with the support of
479 HiLIFE Laboratory Animal Center Core Facility, the University of Helsinki, Finland.
480

481 Funding
482 These studies have been supported by grants by the Academy of Finland (294710, 303124, 307416,
483 327192), Sigrid Jusélius Foundation, Jane & Aatos Erkko Foundation, the Helsinki Institute of Life
484 Science (HiLIFE) Fellow Program, Bilateral exchange program between the Academy of Finland and
485 JSPS (Japan Society for the Promotion of Science), The Finnish Medical Foundation, and Biomedicum
486 Helsinki Foundation.
487

488 Conflict of Interest
489 EC is a co-founder and Board member of Kasvu Therapeutics. The other authors declare no
490 competing financial interests.
491

492 Author Contributions

JU and EC conceived of and designed the project. EJ conducted all experiments including TRAP analysis, immunohistochemistry, imaging, and mitochondrial analysis under the supervision of JU. IS conducted imaging analysis. All authors were involved in writing the manuscript.

References

1. Castrén E, Hen R. Neuronal plasticity and antidepressant actions. Trends Neurosci. 2013;36:259–267.

2. Umemori J, Winkel F, Didio G, Llach Pou M, Castrén E. iPlasticity: Induced juvenile-like plasticity in the adult brain as a mechanism of antidepressants. Psychiatry Clin Neurosci. 2018;72:633–653.

3. Vetencourt JFM, Sale A, Viegi A, Baroncelli L, De Pasquale R, O'Leary OF, et al. The antidepressant fluoxetine restores plasticity in the adult visual cortex. Science (1979). 2008;320:385–388.

4. Karpova NN, Pickenhagen A, Lindholm J, Tiraboschi E, Kulesskaya N, Ágústsdóttir A, et al. Fear Erasure in Mice Requires Synergy Between Antidepressant Drugs and Extinction Training. Science (1979). 2011;334:1731–1734.

5. Jetsonen E, Didio G, Winkel F, Llach Pou M, Boj C, Kuczynski-Noyau L, et al. Activation of TrkB in Parvalbumin interneurons is required for the promotion of reversal learning in spatial and fear memory by antidepressants. Neuropsychopharmacology. 2023. 21 March 2023. https://doi.org/10.1038/S41386-023-01562-Y.

6. Malberg JE, Duman RS. Cell Proliferation in Adult Hippocampus is Decreased by Inescapable Stress: Reversal by Fluoxetine Treatment. Neuropsychopharmacology. 2003;28:1562–1571.

7. Casarotto PC, Girych M, Fred SM, Kovaleva V, Moliner R, Enkavi G, et al. Antidepressant drugs act by directly binding to TRKB neurotrophin receptors. Cell. 2021;184:1299-1313.e19.

8. Sohal VS, Zhang F, Yizhar O, Deisseroth K. Parvalbumin neurons and gamma rhythms enhance cortical circuit performance. Nature. 2009;459:698–702.

9. Bartos M, Vida I, Jonas P. Synaptic mechanisms of synchronized gamma oscillations in inhibitory interneuron networks. Nat Rev Neurosci. 2007;8:45–56.

522 10. Donato F, Rompani SB, Caroni P. Parvalbumin-expressing basket-cell network plasticity
523 induced by experience regulates adult learning. Nature. 2013;504:272–276.

524 11. Winkel F, Ryazantseva M, Voigt MB, Didio G, Lilja A, Llach Pou M, et al. Pharmacological and
525 optical activation of TrkB in Parvalbumin interneurons regulate intrinsic states to orchestrate
526 cortical plasticity. Mol Psychiatry. 2021;26:7247–7256.

527 12. Fawcett JW, Oohashi T, Pizzorusso T. The roles of perineuronal nets and the perinodal
528 extracellular matrix in neuronal function. Nat Rev Neurosci. 2019;20:451–465.

529 13. Kwok JCF, Dick G, Wang D, Fawcett JW. Extracellular matrix and perineuronal nets in CNS
530 repair. Dev Neurobiol. 2011;71:1073–1089.

531 14. Lensjø KK, Lepperød ME, Dick G, Hafting T, Fyhn M. Removal of perineuronal nets unlocks
532 juvenile plasticity through network mechanisms of decreased inhibition and increased gamma
533 activity. Journal of Neuroscience. 2017;37:1269–1283.

534 15. Lesnikova A, Casarotto PC, Fred SM, Voipio M, Winkel F, Steinzeig A, et al. Chondroitinase and
535 antidepressants promote plasticity by releasing TRKB from dephosphorylating control of ptpσ
536 in parvalbumin neurons. Journal of Neuroscience. 2021;41:972–980.

537 16. Pizzorusso T, Medini P, Berardi N, Chierzi S, Fawcett JW, Maffei L. Reactivation of Ocular
538 Dominance Plasticity in the Adult Visual Cortex. Science (1979). 2002;298:1248–1251.

539 17. Ohira K, Takeuchi R, Shoji H, Miyakawa T. Fluoxetine-Induced Cortical Adult Neurogenesis.
540 Neuropsychopharmacology. 2013;38:909–920.

541 18. Mikics É, Guirado R, Umemori J, Tóth M, Biró L, Miskolczi C, et al. Social Learning Requires
542 Plasticity Enhanced by Fluoxetine Through Prefrontal Bdnf-TrkB Signaling to Limit Aggression
543 Induced by Post-Weaning Social Isolation. Neuropsychopharmacology. 2018;43:235–245.

544 19. Ferguson BR, Gao W-J. PV Interneurons: Critical Regulators of E/I Balance for Prefrontal
545 Cortex-Dependent Behavior and Psychiatric Disorders. Front Neural Circuits. 2018;12.

546 20. Frischknecht R, Heine M, Perrais D, Seidenbecher CI, Choquet D, Gundelfinger ED. Brain
547 extracellular matrix affects AMPA receptor lateral mobility and short-term synaptic plasticity.
548 Nat Neurosci. 2009;12:897–904.

549 21. Lesnikova A, Casarotto P, Moliner R, Fred SM, Biojone C, Castrén E. Perineuronal Net Receptor
550 PTPσ Regulates Retention of Memories. Front Synaptic Neurosci. 2021;13.

551 22. Tewari BP, Chaunsali L, Campbell SL, Patel DC, Goode AE, Sontheimer H. Perineuronal nets
552 decrease membrane capacitance of peritumoral fast spiking interneurons in a model of
553 epilepsy. Nat Commun. 2018;9:4724.

554 23. Alaiyed S, McCann M, Mahajan G, Rajkowska G, Stockmeier CA, Kellar KJ, et al. Venlafaxine
555 Stimulates an MMP-9-Dependent Increase in Excitatory/Inhibitory Balance in a Stress Model
556 of Depression. The Journal of Neuroscience. 2020;40:4418–4431.

557 24. Cheng A, Hou Y, Mattson MP. Mitochondria and neuroplasticity. ASN Neuro. 2010;2:243–256.

558 25. Mattson MP. Mitochondrial regulation of neuronal plasticity. Neurochem Res. 2007;32:707–
559 715.

560 26. Wong-Riley MTT. Cytochrome oxidase: an endogenous metabolic marker for neuronal activity.
561 Trends Neurosci. 1989;12:94–101.

562 27. Yano M, Terada K, Mori M. Mitochondrial Import Receptors Tom20 and Tom22 Have
563 Chaperone-like Activity. Journal of Biological Chemistry. 2004;279:10808–10813.

564 28. Kravic B, Harbauer AB, Romanello V, Simeone L, Vögtle F-N, Kaiser T, et al. In mammalian
565 skeletal muscle, phosphorylation of TOMM22 by protein kinase CSNK2/CK2 controls
566 mitophagy. Autophagy. 2018;14:311–335.

567 29. de Oliveira MR. Fluoxetine and the mitochondria: A review of the toxicological aspects. Toxicol
568 Lett. 2016;258:185–191.

569 30. Filipović D, Costina V, Perić I, Stanisavljević A, Findeisen P. Chronic fluoxetine treatment directs
570 energy metabolism towards the citric acid cycle and oxidative phosphorylation in rat
571 hippocampal nonsynaptic mitochondria. Brain Res. 2017;1659:41–54.

572 31. Curti C, Mingattao FE, Polizello ACM, Galastri LO, Uyemura SA, Santos AC. Fluoxetine interacts
573 with the lipid bilayer of the inner membrane in isolated rat brain mitochondria, inhibiting
574 electron transport and F1F0-ATPase activity. Mol Cell Biochem. 1999;199:103–109.

575 32. Hroudová J, Fišar Z. In vitro inhibition of mitochondrial respiratory rate by antidepressants.
576 Toxicol Lett. 2012;213:345–352.

577 33. Agostinho FR, Réus GZ, Stringari RB, Ribeiro KF, Ferreira GK, Jeremias IC, et al. Olanzapine plus
578 fluoxetine treatment alters mitochondrial respiratory chain activity in the rat brain. Acta
579 Neuropsychiatr. 2011;23:282–291.

580 34. Miller EK, Cohen JD. An Integrative Theory of Prefrontal Cortex Function. Annu Rev Neurosci.
581 2001;24:167–202.

582 35. Grace AA, Floresco SB, Goto Y, Lodge DJ. Regulation of firing of dopaminergic neurons and
583 control of goal-directed behaviors. Trends Neurosci. 2007;30:220–227.

584 36. Guirado R, Perez-Rando M, Ferragud A, Gutierrez-Castellanos N, Umemori J, Carceller H, et al.
585 A Critical Period for Prefrontal Network Configurations Underlying Psychiatric Disorders and
586 Addiction. Front Behav Neurosci. 2020;14.

587 37. Sotres-Bayon F, Cain CK, LeDoux JE. Brain Mechanisms of Fear Extinction: Historical
588 Perspectives on the Contribution of Prefrontal Cortex. Biol Psychiatry. 2006;60:329–336.

589 38. Quirk GJ, Mueller D. Neural Mechanisms of Extinction Learning and Retrieval.
590 Neuropsychopharmacology. 2008;33:56–72.

591 39. Bush G, Luu P, Posner MI. Cognitive and emotional influences in anterior cingulate cortex.
592 Trends Cogn Sci. 2000;4:215–222.

593 40. Hippenmeyer S, Vrieseling E, Sigrist M, Portmann T, Laengle C, Ladle DR, et al. A
594 Developmental Switch in the Response of DRG Neurons to ETS Transcription Factor Signaling.
595 PLoS Biol. 2005;3:e159.

596 41. Madisen L, Zwingman TA, Sunkin SM, Oh SW, Zariwala HA, Gu H, et al. A robust and high-
597 throughput Cre reporting and characterization system for the whole mouse brain. Nat
598 Neurosci. 2010;13:133–140.

599 42. Heiman M, Kulicke R, Fenster RJ, Greengard P, Heintz N. Cell type-specific mRNA purification
600 by translating ribosome affinity purification (TRAP). Nat Protoc. 2014;9:1282–1291.

601 43. Emaus RK, Grunwald R, Lemasters JJ. Rhodamine 123 as a probe of transmembrane potential
602 in isolated rat-liver mitochondria: spectral and metabolic properties. Biochim Biophys Acta.
603 1986;850:436–448.

604 44. George Paxinos, Keith B. J. Franklin. The mouse brain in stereotaxic coordinates, 2nd edition.
605 Academic_Press; 2001.

606 45. Love MI, Huber W, Anders S. Moderated estimation of fold change and dispersion for RNA-seq
607 data with DESeq2. Genome Biol. 2014;15:1–21.

608 46. Wu T, Hu E, Xu S, Chen M, Guo P, Dai Z, et al. clusterProfiler 4.0: A universal enrichment tool
609 for interpreting omics data. The Innovation. 2021;2:100141.

610 47. den Brave F, Pfanner N, Becker T. Mitochondrial entry gate as regulatory hub. Biochimica et
611 Biophysica Acta (BBA) - Molecular Cell Research. 2024;1871:119529.

612 48. Vanden Broeck A, Klinge S. Eukaryotic Ribosome Assembly. Annu Rev Biochem. 2024;93:189–
613 210.

614 49. Campos RK, Wijeratne HRS, Shah P, Garcia-Blanco MA, Bradrick SS. Ribosomal stalk proteins
615 RPLP1 and RPLP2 promote biogenesis of flaviviral and cellular multi-pass transmembrane
616 proteins. Nucleic Acids Res. 2020;48:9872–9885.

617 50. Tiganis T, Bennett AM. Protein tyrosine phosphatase function: the substrate perspective.
618 Biochemical Journal. 2007;402:1–15.

619 51. Borovac J, Bosch M, Okamoto K. Regulation of actin dynamics during structural plasticity of
620 dendritic spines: Signaling messengers and actin-binding proteins. Molecular and Cellular
621 Neuroscience. 2018;91:122–130.

622 52. Tucker K, Fadool DA. Neurotrophin modulation of voltage-gated potassium channels in rat
623 through TrkB receptors is time and sensory experience dependent. J Physiol. 2002;542:413–
624 429.

625 53. Rantamäki T, Hendolin P, Kankaanpää A, Mijatovic J, Piepponen P, Domenici E, et al.
626 Pharmacologically Diverse Antidepressants Rapidly Activate Brain-Derived Neurotrophic
627 Factor Receptor TrkB and Induce Phospholipase-Cγ Signaling Pathways in Mouse Brain.
628 Neuropsychopharmacology. 2007;32:2152–2162.

629 54. Fred SM, Laukkanen L, Brunello CA, Vesa L, Göös H, Cardon I, et al. Pharmacologically diverse
630 antidepressants facilitate TRKB receptor activation by disrupting its interaction with the
631 endocytic adaptor complex AP-2. Journal of Biological Chemistry. 2019;294:18150–18161.

632 55. Saarelainen T, Hendolin P, Lucas G, Koponen E, Sairanen M, MacDonald E, et al. Activation of
633 the TrkB Neurotrophin Receptor Is Induced by Antidepressant Drugs and Is Required for
634 Antidepressant-Induced Behavioral Effects. The Journal of Neuroscience. 2003;23:349–357.

635 56. Shi Y. Serine/Threonine Phosphatases: Mechanism through Structure. Cell. 2009;139:468–
636 484.

637 57. Kanai Y, Hediger MA. The glutamate and neutral amino acid transporter family: physiological
638 and pharmacological implications. Eur J Pharmacol. 2003;479:237–247.

639 58. Bar-Peled L, Sabatini DM. Regulation of mTORC1 by amino acids. Trends Cell Biol.
640 2014;24:400–406.

641 59. Tasan RO, Verma D, Herzog H, Sperk G. Neuropeptide Y in the basolateral amygdala
642 modulates the acquisition of conditioned fear. BMC Pharmacol. 2010;10:A33.

643 60. Caillard O, Moreno H, Schwaller B, Llano I, Celio MR, Marty A. Role of the calcium-binding
644 protein parvalbumin in short-term synaptic plasticity. Proceedings of the National Academy of
645 Sciences. 2000;97:13372–13377.

646 61. Schwaller B. The continuing disappearance of “pure” Ca2+ buffers. Cellular and Molecular Life
647 Sciences. 2009;66:275–300.

648 62. Dean C, Liu H, Staudt T, Stahlberg MA, Vingill S, Bückers J, et al. Distinct Subsets of Syt-
649 IV/BDNF Vesicles Are Sorted to Axons versus Dendrites and Recruited to Synapses by Activity.
650 The Journal of Neuroscience. 2012;32:5398–5413.

651 63. Pelkey KA, Barksdale E, Craig MT, Yuan X, Sukumaran M, Vargish GA, et al. Pentraxins
652 Coordinate Excitatory Synapse Maturation and Circuit Integration of Parvalbumin
653 Interneurons. Neuron. 2015;85:1257–1272.

654 64. Alaiyed S, Conant K. A Role for Matrix Metalloproteases in Antidepressant Efficacy. Front Mol
655 Neurosci. 2019;12.

656 65. Minichiello L. TrkB signalling pathways in LTP and learning. Nat Rev Neurosci. 2009;10:850–
657 860.

66. Sohal VS, Rubenstein JLR. Excitation-inhibition balance as a framework for investigating mechanisms in neuropsychiatric disorders. Mol Psychiatry. 2019;24:1248–1257.

67. Marín O. Interneuron dysfunction in psychiatric disorders. Nat Rev Neurosci. 2012;13:107–120.

68. Friedman JR, Nunnari J. Mitochondrial form and function. Nature. 2014;505:335–343.

69. Milad MR, Quirk GJ. Fear Extinction as a Model for Translational Neuroscience: Ten Years of Progress. Annu Rev Psychol. 2012;63:129–151.

70. Duman RS, Sanacora G, Krystal JH. Altered Connectivity in Depression: GABA and Glutamate Neurotransmitter Deficits and Reversal by Novel Treatments. Neuron. 2019;102:75–90.